IARJSET ISSN (O) 2393-8021, ISSN (P) 2394-1588

International Advanced Research Journal in Science, Engineering and Technology

Impact Factor 7.105 ⁜ Vol. 9, Issue 2, February 2022

DOI: 10.17148/IARJSET.2022.9284

Investigation on Mixed Alkali Bismuth-Borate glasses doped with Silver Nanoparticles

Rajeshree Patwari D.[1]*, Dhanalakshmi M.[2], B. Eraiah[3]

[1,2]Department.of Physics, Nrupathunga University, Bangalore-5600001, Karnataka

[3]Department.of Physics, Bangalore University, Bangalore-5600056, Karnataka

Abstract: The mixed alkali Bi-borate glasses with different concentrations of silver nitrate were produced by the melt-quenching method. The molar concentrations of silver were varied from 0.0 to 0.5mol% in steps of 0.1mol% and annealed at 300 degrees for two hours. The samples were characterized by powdered x-ray diffraction to conform the non-crystalline environment of the samples. The densities of the glasses were measured by the Archimedes principle. The glass sample were studies by the UV-Visible absorption spectroscopy. The formation of silver nanoparticles was indicated by the absorption band witnessed in the absorption spectra known as surface plasmon band. The plasmon band changes with the concentrations of silver doping. The silver nanoparticles in the glass environment were also confirmed by the transmission electron microscopy. The direct and indirect band gap valued were in the range 2.972-3.08eV and 1.786-2.782eV respectively. The Urbach energies and densities were found to change in similar way with the doping concentration but Urbach energy and the band gap energies were found to vary exactly in opposite manner. The plasmon band found was more sharp for less silver doping and with silver doping the band became more broad. The plasmon band formed due to the silver nanoparticles may be used to enhance the luminescence property of luminescent ions by making use of the plasmon resonance phenomenon.

Keywords: Silver Nanoparticles, Melt quenching, Surface Plasmon Resonance

1. INTRODUCTION

Heavy metals doped glasses have properties like higher transparency, higher refractive index, and higher optical nonlinear susceptibility [1-3]. High density, heavy metal cation impart radiation shielding ability to the glasses. [4]. Above all rare earth doping brands the glasses as luminescent glasses mainly used in the applications like solid state lasers and also optical amplifier [5-6].

Recent research focus on the bismuth doped glasses attracted great attention as they are used in a wide area of applications. These glasses are characterized not only by exclusive properties like high refractive index, high density but also high relative permeability, enlarged transmission in IR region. Bismuth oxide is a glass modifier, alone cannot form glasses because of its low field strength but along with a good glass former forms glasses with a wide range of compositions. Another most important advantage is that the dangerous effect of lead on ecology and environment may eliminated by replacing lead with bismuth [7]. B_2O_3 oxide is main and easily glass forming component with lower melting point and good thermal stability and high transparency. The smaller size of B^{3+} ions offers high bond strength and can change its oxidation state easily from B^{3+} to B^{4+} [8]. The alkali metal oxides when added to the glass matrix modify the structure and thermal properties of the glasses by creating non-bridging oxygen atoms. The ease of synthesis of bismuth doped borate glasses lie in its lower melting point [8]. It was reported silver nanoparticles were created in Pr3+ doped tellurite glasses for laser illumination [9]. Many glasses were reported with silver nanoparticles for enhancement of luminescence. Silver nanoparticles were also produced and studied in Phosphate glasses [10]. Comparatively not much work was reported with borate glasses with metal nanoparticles hence our research aims to create silver nanoparticles in bismuth borate glasses doped with alkali oxides and study its optical properties.

2. EXPERIMENTAL PROCEDURE AND CHARACTERIZATION

2.1 Synthesis of glasses: The materials used for the synthesis of the samples were extra pure Analytical reagent (AR) grade chemicals with the composition (65-x) B_2O_3-10Bi_2O_3-10Na_2O-15 K_2O-x$AgNO_3$ (where x changes from 0.0 to 0.5 in steps of 0.1 mol %) All the materials involved were weighed accurately, powdered and mixed thoroughly and then heated in the muffle furnace till a clear melt is formed with frequent stirring. At around 1000^oC after ensuring the formation of perfect melt without any bubbles the melted fluid is suddenly poured between brass moulds. The samples were annealed at 300^0C for two hours in order to remove the thermal strain retained by the sample due to sudden cooling by melt quenching. The samples were powdered and polished for different studies depending on the requirement for the

IARJSET ISSN (O) 2393-8021, ISSN (P) 2394-1588

International Advanced Research Journal in Science, Engineering and Technology

Impact Factor 7.105 ⁜ Vol. 9, Issue 2, February 2022

DOI: 10.17148/IARJSET.2022.9284

characterization and labelled as B1, B2, B3, B4, B5 and Base with increasing concentration of silver nitrate from 0.1, 0.2, 0.3, 0.4, 0.5mol% and the base glass without silver nitrate.

2.2 Characterization: The physical properties like density by Archimedes principle and the structural properties were characterised by the Powdered X-ray diffraction using Rigaku Ultima iv X-ray diffractometer with Cu Kα with λ=1.54059292 A^0 and Scan speed- 2°min^{-1}, 2θ ranging from 20 to 80°. The Optical properties were studied by the Shematzu UV-Visible spectrometer having wavelength range 200-1100nm with double beam. Nanoparticles were confirmed their distribution, size and shape were analysed by the Transmission electron microscopy Jeol/JEM 2100.

3. RESULTS AND DISCUSSION

3.1 XRD analysis: The samples are amorphous solids, which is confirmed by the X-ray diffraction pattern shown in fig 1. In the x-ray diffraction has no sharp peaks instead two humps centred around 28^0 and 45^0 were observed which confirms the non-crystalline arrangements of the molecules [11].

3.2 Density: The density which is material property can be determined by Standard principle of Archimedes [12,13]. Weight in air and weight in toluene is recorded. Toluene is used for immersing the sample.

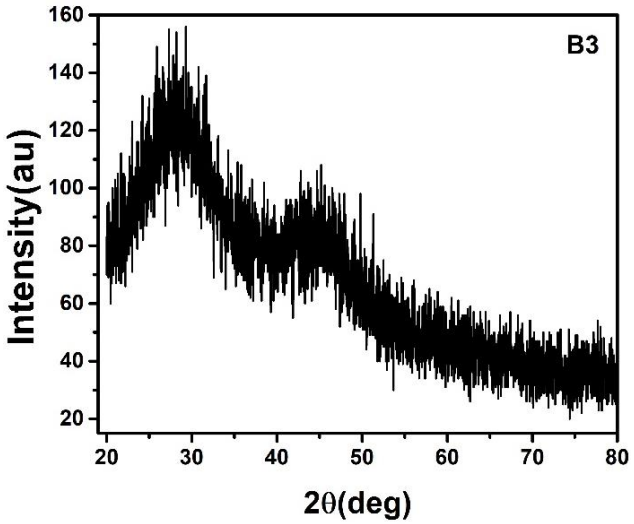

Figure 1. XRD pattern of B3 glass

Density of the glass $\rho = \frac{W_a}{(W_a - W_l)} \rho_l$ ……..(1)

where

ρ_l is the density of immersing liquid

W_a is the weight of glass in air

W_l is the weight of glass in air

The molar volume V_m=Molar mass/density……. (2)

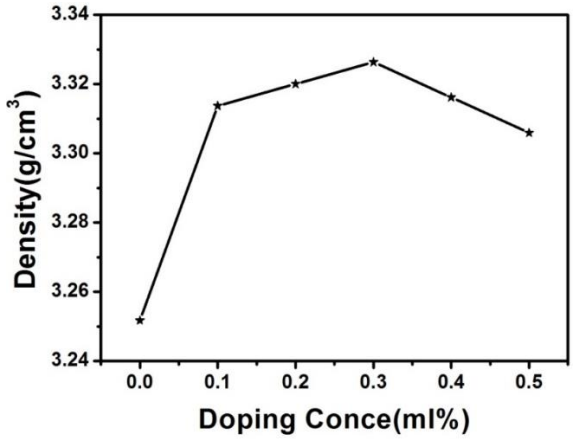

Figure 2. Behaviour of density with silver doping

IARJSET ISSN (O) 2393-8021, ISSN (P) 2394-1588

International Advanced Research Journal in Science, Engineering and Technology

Impact Factor 7.105 ⁜ Vol. 9, Issue 2, February 2022

DOI: 10.17148/IARJSET.2022.9284

The density of a substance depends on the material and most of the other properties depend on this fundamental material property. The variation of density with the silver doping was as displayed in the fig 2. The density of the glasses increases with silver doping and then decreases after 0.3mol% of doping. The maximum density indicates more number of bridging oxygen atoms was formed and the structure becomes more compact. Base glass was found to show the least density.

3.3 The UV-Visible Absorption Studies:

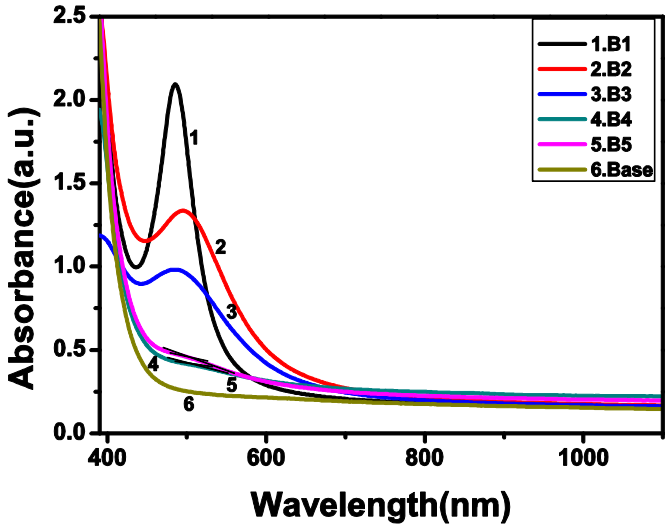

Figure 3. UV-visible absorption spectra of base and silver doped bismuth borate glasses

The UV-Visible spectra are shown in the fig 3. The Base glass without silver doping showed almost no absorption when the wavelength is decreased from 1100nm to around 700nm and then increased gradually and drastically in the UV region. The same thing also true with the other samples and in addition to this a characteristic peak is observed in the samples B1 to B5. This peculiar peak is due to the formation of silver nanoparticles known as surface plasmon resonance absorption band(SPR) [14]. This absorption band is due to the collective oscillation of silver nanoparticles. The band is centred around 485, 494, 490, 505, 506nm for different concentrations. With increase in silver doping the band centre is found to red shift. This phenomenon shown by the silver nanoparticles may be utilized to increase to increase the luminescence of rare earth ions (RE ions) either by the direct transfer of energy from SNPs to RE ions or by the enhanced electric field near RE ions because of SPR of SNPs.

The optical band gap of the amorphous solids may be determined by using Mott and Davis [15]. In this model the absorption coefficient is calculated with absorbance and sample thickness

$$\alpha = 2.303 \log ({}^{A}/_{d}) \quad \ldots\ldots (3)$$

The absorption coefficient depends on the band to band transition energy by the relation (16)

$$\alpha(\nu) = ({}^{B}/_{h\nu})(h\nu - E_{opt})^{n} \quad \ldots\ldots (4)$$

where B is a constant,
hν is the energy of photon
E_{opt} is the optical energy
n is the exponent equal to ½ and 2 for direct and indirect transitions respectively.
The refractive index of the material may be determined equation [17]

$$\left(\frac{n^2-1}{n^2+2}\right) = 1 - \sqrt{{}^{Eg}/_{20}} \quad \ldots\ldots (5)$$

IARJSET ISSN (O) 2393-8021, ISSN (P) 2394-1588

International Advanced Research Journal in Science, Engineering and Technology

Impact Factor 7.105 ⁜ Vol. 9, Issue 2, February 2022

DOI: 10.17148/IARJSET.2022.9284

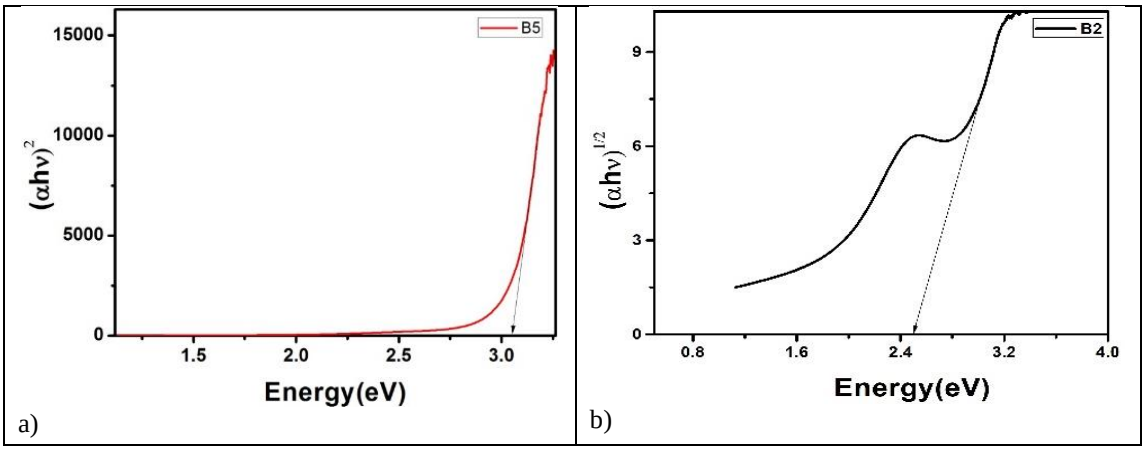

Figure 6 Tauc plots for the determination of a) Direct b) Indirect band gap energies

The fig 6a and 6b were used to find the band gap energies. The glasses best fits for both direct and indirect energy gaps. The direct and indirect band gap energies were calculated by the intercept formed in the plots of $(\alpha h\nu)^2$ and $(\alpha h\nu)^{1/2}$ against incident energy (Tauc plots) respectively.

The direct and indirect transition were due to photon and phonon absorptions respectively were found to decrease and then after 0.3 mol% increases and changes exactly like that of density of the glasses with doping. When the medium is denser, the energy levels come close and the band gap energy decreases and visa-versa. And at the same time the Urbach energy increases and then decreases. As the refractive index is directly proportional to the density varies similarly with the density.

The formulae used for the calculation of the optical properties are

i) Dielectric Constant, $\epsilon = n^2$

ii) Molar Reflectivity, $R_m = V_m \ (\epsilon - 1)/(\epsilon - 2)$

iii) Polarizability, $\alpha = 3R_m/(4\pi N_A)$

iv) No. of silver ions $N_{Ag} = x\rho N_A/M_m$

v) Polaron Radii $r_p = (1/2)(\pi/6N)^{1/3}$

vi) Distance between Ag-Ag $d_{Ag-Ag} = (1/N)^{1/3}$

vii) Susceptibility $\chi = (n^2 - 1)/4\pi$

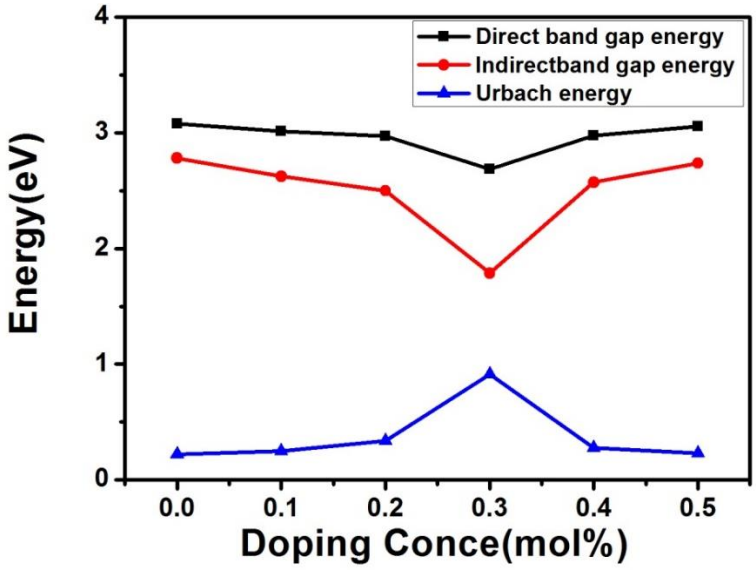

Figure 7. Variation of band gap and Urbach energies with silver doping

IARJSET ISSN (O) 2393-8021, ISSN (P) 2394-1588

International Advanced Research Journal in Science, Engineering and Technology

Impact Factor 7.105 ⁜ Vol. 9, Issue 2, February 2022

DOI: 10.17148/IARJSET.2022.9284

Table 1. The physical and optical properties of the glasses

Glass Codes / Properties	B1	B2	B3	B4	B5
Doping Concentration (Ag)	0.1	0.2	0.3	0.4	0.5
Density(g/cm^3)	3.314	3.320	3.326	3.316	3.306
Molar Volume(cm3) V_m	47.79	47.71	47.63	47.79	47.96
Direct band gap energy(eV)	3.014	2.972	2.687	2.978	3.055
Indirect Band gap energy(eV)	2.623	2.499	1.786	2.572	2.736
Urbach Energy	0.248	0.339	0.914	0.275	0.230
Ref.ind (D)	2.393	2.405	2.487	2.403	2.382
Ref Ind(I)	2.507	2.547	2.835	2.523	2.472
Molar Mass(g)	158.35	158.40	158.44	158.49	158.54
Dielectric Constant ϵ	5.728	5.782	6.185	5.775	5.675
Polarizability $\alpha(10^{-23})$	1.159	1.162	1.196	1.163	1.158
No of Silver ions N (10^{21})	1.260	2.525	3.793	5.041	6.280
Distance between Ag ions(10^{-8})	9.258	7.344	6.412	5.832	5.420
Susceptibility χ	0.3762	0.3805	0.4125	0.3799	0.3720
Metallization=(1-Rm/Vm)	0.3882	0.3855	0.3665	0.3859	0.3909

The physical optical properties were tabulated in the table 1. The variation of direct and indirect band gap energies was displayed in the fig 5. Both the energies vary similarly first decreases and attains minimum at 0.3 mol% of silver doping later increases with silver doping. A plot of ln absorption coefficient against energy is employed to determine the Urbach energy. The disorder is measured as Urbach energy obtained by the reciprocal of the slope in absorption edge. The disorder first increases and then decreases with silver doping. The behaviour of direct band gap energy and density variation with silver is plotted in the figure. They vary exactly oppositely with doping.

3.4 TEM analysis

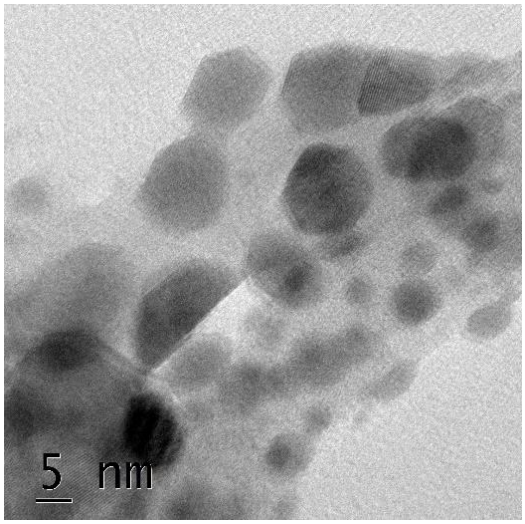

Figure 4. TEM image of B1 glass

The silver nanoparticles were observed and confirmed by the TEM image shown in the fig 4. The shape of the particles observed to be hexagonal and the sizes of the particles are not same. The particles size is found in the range 3 to 17nm which shown in the fig 5. The ImageJ software is used for the size measurement and the average size of the SNP was obtained to be 6.791≈ 7nm.

IARJSET ISSN (O) 2393-8021, ISSN (P) 2394-1588

International Advanced Research Journal in Science, Engineering and Technology

Impact Factor 7.105 ⁜ Vol. 9, Issue 2, February 2022

DOI: 10.17148/IARJSET.2022.9284

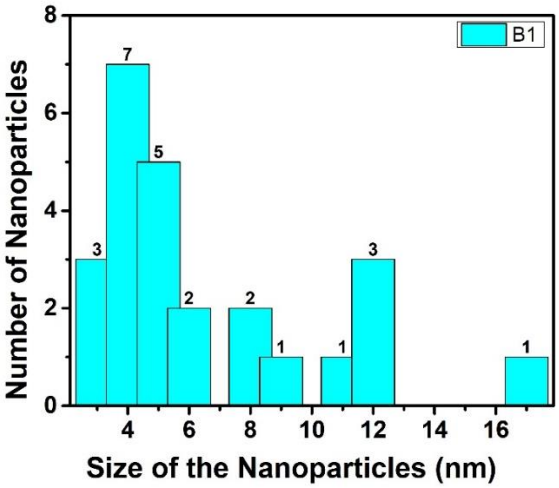

Figure 5. The bar graph showing the nanoparticles' size distribution

This band (SPR) is sharper and more intense for lesser doping and becomes broader and less intense with increasing doping of silver. The band shifts to higher wavelength with increased doping which also indicates the formation of bigger sized nanoparticles. The band also broadens due to non- uniform size of the nanoparticles.

4. CONCLUSIONS:

Bismuth and Mixed alkali borate glasses were prepared with different molar concentrations of silver nitrate by melt quenching. Amorphous nature was established by the x-ray diffraction After annealing the glasses silver nanoparticles were produced in the glass matrix.

The plasmon band observed in the UV-Visible spectra indicates the formation of silver nanoparticles. SNPs formation was also confirmed by the TEM analysis. These silver nanoparticles may produce the luminescence enhancement luminescent centers such as RE ions if the glasses were doped with them.

REFERENCES:

1. Ram, S., Bahadur, D. & Chakravorty, D. "Crystallisation of W-type hexagonal ferrites in an oxide glass with As2O3 as nucleation catalyst". J. Magn. Magn. Mater. 67, 378, 1987 doi: 10.1016/j.ceramint.2004.12.008
2. Ram, S., Chakravorty, D. & Bahadur, D. "Effect of nucleating agents on the crystallisation behaviour of barium hexaferrite in a borate glass". J. Magn. Magn. Mater. 62, 221,1986 https://doi.org/10.1016/0304-8853(86)90148-4
3. Ram, S. & Ram, K. "Infrared reflectance spectra and formalism of precipitation of acicular magnetic particles in network glasses". Infrared Phys. Technol. 37, 457,1996 doi:10.1016/1350-4495(95)00079-8
4. Kumar, A., Jain, A., Sayyed, M. I., Laariedh, F., Mahmoud, K. A., Nebhen, J., Faruque, "M. R. I. Tailoring bismuth borate glasses by incorporating PbO/GeO2 for protection against nuclear radiation". Scientific Reports, 11(1). 2021 doi:10.1038/s41598-021-87256-1
5 K. Swapna, Sk Mahamuda, A. Srinivasa Rao, M. Jayasimhadri, T. Sasikala and L. Rama Moorthy, "Visible fluorescence characteristics of Dy3+ doped zinc alumino bismuth borate glasses for optoelectronic devices", Ceram. Interfaces, 39, 8459–8465, 2013 doi: 10.1016/j.ceramint.2013.04.028
6 K. Swapna, S. Mahamuda, A. Srinivasa Rao, M. Jayasimhadri, S. Shakya and G. Vijaya Prakash, "Tb3+ doped Zinc Alumino Bismuth Borate glasses for green emitting luminescent devices" J. Luminescence, 156, 180–187, 2014 doi:10.1016/j.jlumin.2014.08.019
7. An, J-S., Park, J-S., Kim, J-R., & Hong, K. S. "Effects of Bi2O3 and Na2O on the Thermal and Dielectric Properties of Zinc Borosilicate Glass for Plasma Display Panels". J. Am. Ceram. Soc., 89, 3658-3661,2006. doi:10.1111/j.1551-2916.2006. 01309.x
8. Sayyed, M. I. et al." Investigation on gamma and neutron radiation shielding parameters for BaO/SrO–Bi2O3–B2O3 glasses". Radiat. Phys. Chem. 145, 26–33, 2018. doi: 10.1016/j.radphyschem.2017.12.010
9. Hua, Chenxiao; Zhao, Xin; Bun Pun, Edwin Yue; Lin, Hai "Pr3+ doped tellurite glasses incorporated with silver nanoparticles for laser illumination". RSC Advances, 7(88), 55691–55701, 2017. doi:10.1039/c7ra11594f
10. Soltani, I.; Hraiech, S.; Horchani-Naifer, K.; Elhouichet, H.; Férid, M. "Effect of silver nanoparticles on spectroscopic properties of Er3+ doped phosphate glass". Optical Materials, 46, 454–460, 2015. doi: 10.1016/j.optmat.2015.05.003

DOI: 10.17148/IARJSET.2022.9284

11. Sharma, Vandana "Synthesis and Optical Characterization of Silver Doped Sodium Borate Glasses, New Journal of Glass and Ceramics,2(4),111–115, 2012. doi:10.4236/njgc.2012.24019
12. F. Zaman, J. Kaewkhao, G. Rooh , N. Srisittipokakun, H.J. Kim, " Optical and luminescence properties of Li_2O—Gd_2O_3—MO—B_2O_3—Sm_2O_3 (MO=Bi_2O_3, BaO) glasses" Journal of Alloys and Compounds. 676, 275-285, 2016. doi.org/10.1016/j.jallcom.2016.03.176
13. Shoaib, M.; Rooh, G.; Rajaramakrishna, R.; Chanthima, N.; H.J.Kim, ; Tuscharoen, S.; Kaewkhao, J. (2019). "Physical and luminescence properties of samarium doped oxide and oxyfluoride phosphate glasses. Materials Chemistry and Physics", (), S0254058419302160 doi: 10.1016/j.matchemPhys.2019.03.016
14. Chen, Feifei; Cheng, Junwen; Dai, Shixun; Xu, Zhe; Ji, Wei; Tan, Ruiqin; Zhang, Qinyuan "Third-order optical nonlinearity at 800 and 1300 nm in bismuthate glasses doped with silver nanoparticles". Optics Express, 22(11), 13438, 2014. doi:10.1364/OE.22.013438
15. K.F. Mott, E.A. Davis, Electronic processes in non-crystalline materials, Clarendon Press, 1979
16. Lee, S., Hwang, S., Cha, M., Shin, H., & Kim, H. (2008). "Role of Copper Ion in Preventing Silver Nanoparticles Forming in Bi2O3–B2O3–ZnO Glass". J. Phys. Chem. Solids, 69, 1498-1500, 2008. doi.org/10.1016/j.jpcs.2007.10.118
17. V. Dimitrov, S. Sakka, "Electronic oxide polarizability and optical basicity of simple oxides. I" J. Appl. Phys. 79 (3),1736, 1996. doi.org/10.1063/1.360962

